

# FaceXFormer: A Unified Transformer for Facial Analysis

Kartik Narayan\*, Vibashan VS\*, Rama Chellappa, and Vishal M. Patel

Johns Hopkins University

{knaraya4, vvishnu2, rchella4, vpatel136}@jhu.edu  
[https://kartik-3004.github.io/faceformer\\_web/](https://kartik-3004.github.io/faceformer_web/)

**Abstract.** In this work, we introduce *FaceXformer*, an end-to-end unified transformer model for a comprehensive range of facial analysis tasks such as face parsing, landmark detection, head pose estimation, attributes recognition, and estimation of age, gender, race, and landmarks visibility. Conventional methods in face analysis have often relied on task-specific designs and preprocessing techniques, which limit their approach to a unified architecture. Unlike these conventional methods, our *FaceXformer* leverages a transformer-based encoder-decoder architecture where each task is treated as a learnable token, enabling the integration of multiple tasks within a single framework. Moreover, we propose a parameter-efficient decoder, FaceX, which jointly processes face and task tokens, thereby learning generalized and robust face representations across different tasks. To the best of our knowledge, this is the first work to propose a single model capable of handling all these facial analysis tasks using transformers. We conducted a comprehensive analysis of effective backbones for unified face task processing and evaluated different task queries and the synergy between them. We conduct experiments against state-of-the-art specialized models and previous multi-task models in both intra-dataset and cross-dataset evaluations across multiple benchmarks. Additionally, our model effectively handles images "in-the-wild," demonstrating its robustness and generalizability across eight different tasks, all while maintaining the real-time performance of 37 FPS.

## 1 Introduction

Face analysis is a crucial problem as it has broad range of application such as face verification and identification [61, 62], surveillance [19], face swapping [11], face editing [92], de-occlusion [79], 3D face reconstruction [75], retail [1], image generation [78] and face retrieval [81]. Facial analysis tasks (Figure 1 involve face parsing [25, 73], landmarks detection [39, 90], head pose estimation [10, 89], facial attributes recognition [46, 48], age/gender/race estimation [6, 37] and landmarks visibility prediction [31, 43]. Therefore, developing a generalized and robust face model for all tasks is a crucial and longstanding problem in the face community.

---

\* Equal contribution



**Fig. 1:** *FaceXformer* an end-to-end unified transformer model for 8 different facial analysis tasks such as face parsing, landmark detection, head pose estimation, attributes recognition, and estimation of age, gender, race, and landmarks visibility.

In recent years, significant advancements have been made in facial analysis, developing state-of-the-art methods for various tasks [10, 11, 37, 79, 89, 90]. Despite these methods achieving promising performance, they cannot be integrated into a single pipeline due to their specialized model designs and task-specific pre-processing techniques. This limitation hinders the expansion toward developing a single unified model capable of solving all facial analysis tasks (see Table.1). A single model capable of addressing multiple facial analysis tasks is desirable because it: (1) learns a robust and generalized face representation capable of handling in-the-wild images; (2) can model the intra-task relationship (e.g., the relationship between face parsing and landmark detection); and (3) improves task synergy leading to overall performance enhancement. In this work, we introduce *FaceXformer*, an end-to-end unified model designed for a comprehensive range of facial analysis tasks, such as face parsing, landmark detection, head pose estimation, attributes recognition, age/gender/race estimation and landmarks visibility prediction.

*FaceXformer* enables task unification by leveraging the transformer as its core component. Specifically, we introduce a transformer-based encoder-decoder structure, treating each facial analysis task as a unique, learnable token within the framework. Treating each task as a token allows for the simultaneous processing of multiple facial analysis tasks, overcoming the challenges present in conventional methods that depend on separate, task-specific models and pre-processing routines. Furthermore, we introduce a parameter-efficient decoder, FaceX, which processes both face and task tokens together, enabling the model to learn robust face representations that generalize across various tasks. After modeling the intra-task and face-token relationships in the FaceX decoder, the

Methods	FP	LD	HPE	Attr	Age	Gen	Race	Vis	MD	Task Queries	Shared Model
EAGR [65]	✓										
AGRNET [64]	✓										
DML-CSR [87]	✓										
FP-LIIF [56]	✓										
Wing [17]		✓									
SBR [14]		✓									
DeCaFa [12]		✓									
HRNet [69]		✓									
STAR Loss [90]		✓									
FDN [83]			✓								
WHENet [89]			✓								
TriNet [7]			✓								
img2pose [2]			✓								
TokenHPE [82]			✓								
SSP+SSG [26]	✓			✓							
SSPL [58]				✓							
Hetero-FAE [21]				✓	✓	✓	✓		✓		✓
FairFace [27]					✓	✓	✓				
MiVOLO [32]					✓	✓					
MTL-CNN [97]		✓		✓					✓		✓
ProS [13]	✓	✓		✓							
FaRL [88]	✓	✓		✓	✓	✓					
HyperFace [51]		✓	✓			✓		✓	✓		✓
AllinOne [52]		✓	✓		✓	✓		✓	✓		✓
<b>FaceXFormer</b>	✓	✓	✓	✓	✓	✓	✓	✓	✓	✓	✓

**Table 1:** Comparison with representative methods under different task settings. Our proposed *FaceXFormer* can perform various facial analysis tasks in single model. FP - Face Parsing, LD - Landmarks Detection, HPE - Head Pose Estimation, Attr - Attributes Recognition, Age - Age Estimation, Gen - Gender Estimation, Race - Race Estimation, Vis - Landmarks Visibility Prediction, MD - Multi-dataset Training

task tokens are fed into a unified head, which essentially converts these task tokens into corresponding task predictions. We conduct experiments against state-of-the-art specialized models, and previous multi-task models, including both intra-dataset and cross-dataset evaluations across multiple benchmarks. Additionally, we performed extensive experiments to evaluate different task queries and the synergy between them and further experimented with the backbone to assess its effectiveness towards a unified model. Moreover, we show that our model effectively handles images 'in the wild,' demonstrating its robustness and generalizability across eight different tasks. To the best of our knowledge, this is the first work to propose a single model capable of handling all these facial analysis tasks using transformers, all while maintaining real-time performance at 37 FPS. In summary, our paper's contributions are as follows:

1. We introduce *FaceXFormer*, a unified transformer-based framework for the simultaneous processing of multiple facial analysis tasks, eliminating the need for separate, task-specific models.
2. We propose the *FaceX* decoder, a parameter-efficient decoder that treats each facial analysis task as a token and processes them together, leading to improved generalization and task synergy across various tasks.

3. We conducted extensive experiments and analysis, including both intra-dataset and cross-dataset evaluations, comparing our approach to existing state-of-the-art specialized models and multi-task models across all eight tasks.

## 2 Related Work

**Facial analysis tasks:** Facial analysis tasks involve face parsing [9,25,65,73,87], landmarks detection [33,36,39,44,90], head pose estimation [10,67,82,89], facial attributes recognition [46,48,58,88], age/gender/race estimation [6,32,35,37] and landmarks visibility prediction [31,43]. These tasks hold significance in various applications such as face swapping [11], face editing [92], de-occlusion [79], 3D face reconstruction [75], driver assistance [47], human-robot interaction [59], retail [1], face verification and identification [61,62], image generation [78], image retrieval [81] and surveillance [19]. Specialized models excel in their respective tasks but cannot be easily integrated with other tasks due to the need for extensive task-specific pre-processing [40,90]. Generally, these models under-perform when applied to tasks beyond their specialization as their design is specific to their designated tasks. Some works [24,45,84,86] perform multiple tasks simultaneously but utilize the additional tasks for guidance or auxiliary loss calculation to enhance the performance of the primary task. HyperFace [51] and AllinOne [52] are the only studies that explore multi-task learning with the aim of performing multiple tasks, but tend to limit their scope to tasks that inherently complement each other. For instance, landmark detection and head pose estimation are both regression-based tasks that effectively support each other. HyperFace utilizes multi-scale features from different layers of CNNs, and is capable of landmarks detection, head pose estimation and gender estimation, while AllinOne additionally performs face recognition and age estimation. Both these works, misleadingly suggest that they perform face detection, however, they use the selective search [55] algorithm in R-CNN [20] for region proposal, and merely predict whether the selected region is a face.

**Unified transformer models:** In recent years, the rise of transformers [15,68] have paved the way for the unification of multiple tasks within a single architecture. Unified transformer architectures are being explored across various computer vision problems, including segmentation [38,98], visual question answering (VQA) [70,80], tracking [71,91], detection [72]. While these models may not achieve state-of-the-art (SOTA) performance and may under-perform compared to specialized models, they demonstrate satisfactory performance across a variety of tasks. Such unification efforts have led to the development of foundational models like SAM [30], CLIP [49], LLaMA [66], GPT-3 [4], DALL-E [50], etc. However, these models are computationally intensive and not suitable for facial analysis applications that require real-time performance. Motivated by this challenge, we propose *FaceXFormer*: the first lightweight, transformer-based model capable of performing multiple facial analysis tasks. *FaceXFormer* delivers real-

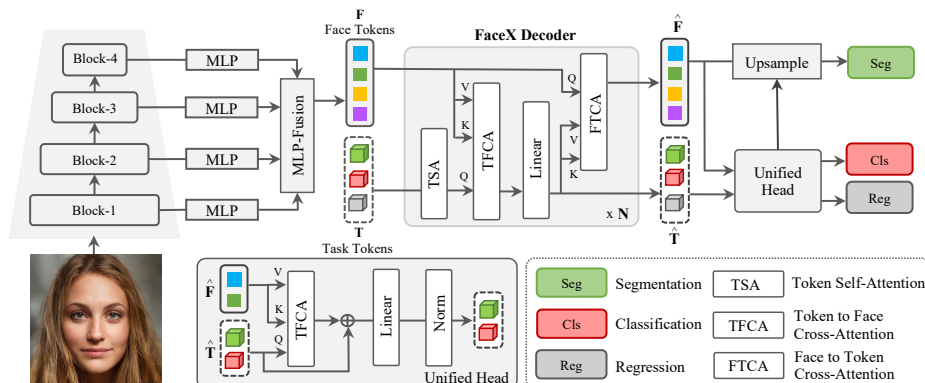


**Fig. 2:** Overview of our proposed framework. The *FaceXFormer* employs an encoder-decoder architecture, extracting multi-scale features from the input face image  $I$ , and fusing them into a unified representation  $F$  via MLP-Fusion. Task tokens  $T$  are processed alongside face representation  $F$  in the FaceX Decoder **FXDec**, resulting in refined task-specific tokens  $\hat{T}$ . These refined tokens are then used for task-specific predictions by passing through the unified head.

time performance at 37 FPS and can be integrated with existing face detectors to provide additional insights about the person of interest.

### 3 Proposed Work

#### 3.1 FaceXFormer

In our framework, we follow a standard encoder-decoder structure as illustrated in Fig. 2. For an input face image  $I \in \mathbb{R}^{H \times W \times 3}$ , we extract coarse to fine-grained multi-scale features  $S_i$ , where  $i$  belongs to the  $i$ -th encoder output. To learn a unified face representation  $F$ , these multi-scale features are then fused using a lightweight MLP-Fusion  $M$  module. Following fusion, we initialize a series of task-specific tokens  $T = \langle T_1, \dots, T_n \rangle$ , with each  $t_i$  representing a face task. Afterward, we initialize task tokens  $T = \langle T_1, \dots, T_n \rangle$ , where  $T_i$  denotes each task. Face tokens  $F$  and task tokens  $T$  are then processed by a Parameter-efficient Decoder **FXDec** where the task tokens are attended with face tokens to learn relevant task representation.

$$\langle \hat{T} \rangle = \mathbf{FXDec}(\langle F, T \rangle; S_i) \quad (1)$$

where,  $\hat{T}$  is the output task tokens. Later these output task tokens are fed into unified heads, where each task token is refined and passed to the task head for corresponding task prediction.

#### 3.2 Multi-scale Encoder

In the encoder, we employ a multi-scale encoding strategy to address the varying feature requirements intrinsic to each face analysis task. For instance, age

estimation requires a global representation, while face parsing necessitates a fine-grained representation. Given an input image  $\mathbf{I}$ , it is processed through a set of encoder layers. For each encoder layer, the output captures information at varying levels of abstraction and detail, generating multi-scale features  $\{\mathbf{S}_i\}_{i=1}^n$ , where  $i$  ranges from 1 to 4. This results in a hierarchical structure of features, wherein each feature map  $\mathbf{S}_i$  transitions from a coarse to a fine-grained representation suitable for diverse facial tasks.

**Lightweight MLP-Fusion:** Assigning each feature-map  $\mathbf{S}_i$  to each face task is sub-optimal; rather, learning a unified face representation is more optimal and parameter-efficient. Following [77], we utilize a Lightweight MLP-Fusion module  $\mathbf{M}$  to generate a fused face representation from the multi-scale features  $\{\mathbf{S}_i\}_{i=1}^n$ . In this framework, each feature map  $\mathbf{S}_i$  is initially passed through a separate MLP layer, standardizing the channel dimensions across scales to facilitate fusion. The transformed features are then concatenated and passed through a fusion MLP layer to aggregate a fused representation  $\mathbf{F}$  as follows:

$$\begin{aligned}\hat{\mathbf{S}}_i &= \text{MLP}_{\text{proj}}(D_i, D_t)(\mathbf{S}_i), \forall i \in \{1, \dots, n\}, \\ \mathbf{F}_{\text{cat}} &= \text{Concat}(\hat{\mathbf{S}}_1, \hat{\mathbf{S}}_2, \dots, \hat{\mathbf{S}}_n), \\ \mathbf{F} &= \text{MLP}_{\text{fusion}}(nD_t, D_t)(\mathbf{F}_{\text{cat}}),\end{aligned}$$

where  $D_i$  and  $D_t$  are the multi-scale feature channel dimensions of  $\mathbf{S}_i$  and the target channel dimension, respectively. The Lightweight MLP-Fusion design ensures minimal computational overhead while maintaining the ability to perform efficient feature fusion, crucial for subsequent face analysis tasks.

### 3.3 FaceX Decoder

Detection transformer (DETR) [8] employs object tokens to learn bounding box predictions for each object. Inspired by this approach, we introduce Task Tokens, whereby each task token is designed to learn specific facial tasks leveraging the fused face representation. However, existing decoders such as DETR [8] and Deformable-DETR [95] are computationally intensive, impacting runtime significantly. To address this, we propose a FaceX (**FXDec**) a parameter-efficient decoder designed to efficiently model the task tokens with face tokens. Specifically, each task token learns a task-related representation by interacting with other task tokens  $\mathbf{T}$  and face tokens  $\mathbf{F}$ , enhancing the overall representation. The Parameter-Efficient Decoder comprises three main components: 1) Task Self-Attention, 2) Task-to-Face Cross-Attention, and 3) Face-to-Task Cross-Attention as illustrated in Fig. 2.

**Task Self-Attention (TSA):** The Task Self-Attention module is designed to refine the task-specific representations within the set of task tokens  $\mathbf{T} = \langle T_1, \dots, T_n \rangle$ . Each task token  $T_i$  is an embedded representation that corresponds to a specific facial task. In TSA, each  $T_i$  is updated by attending to all other task

tokens to capture task-specific interactions. Formally, the updated task token  $T'_i$  is computed as:

$$\mathbf{T}'_i = \text{SelfAttn}(\mathbf{Q} = T'_i, \mathbf{K} = \mathbf{T}, \mathbf{V} = \mathbf{T}), \quad (2)$$

where Attention denotes the multi-headed self-attention mechanism, and  $\mathbf{Q}$ ,  $\mathbf{K}$ , and  $\mathbf{V}$  represent the queries, keys, and values, respectively. Therefore, TSA essentially helps to model the inter-task relationship and improve overall task synergy.

**Task-to-Face Cross-Attention (TFCA):** The Task-to-Face Cross-Attention module allows each task token to interact with the fused face representation  $\mathbf{F}$ . This enables each task token to gather information relevant to its specific facial task from the fused face features. In this module, the fused face representation  $\mathbf{F}$  acts as both key and value, while the task tokens serve as queries. The updated task token  $\hat{T}_i$  is then computed as follows:

$$\hat{T}_i = \text{CrossAttn}(\mathbf{Q} = T'_i, \mathbf{K} = \mathbf{F}, \mathbf{V} = \mathbf{F}), \quad (3)$$

where  $\hat{\mathbf{T}} = \langle \hat{T}_1, \dots, \hat{T}_n \rangle$  is the output task token. Thus, TFCA enables direct interaction between the task-specific tokens and the compact facial features, facilitating task-focused feature extraction.

**Face-to-Task Cross-Attention (FTCA):** Conversely, the Face-to-Task Cross-Attention module is designed to refine the fused face representation  $\mathbf{F}$  based on the information from the updated task tokens. This process aids in enhancing the face representation with task-specific details, thereby improving the extraction of overall fused representation. In FTCA, the set of updated task tokens  $\mathbf{T}' = \{\mathbf{T}'_1, \mathbf{T}'_2, \dots, \mathbf{T}'_m\}$  acts as both keys and values, while the fused face features  $\mathbf{F}$  serve as queries. The refined face representation  $\hat{\mathbf{F}}$  is computed as:

$$\hat{\mathbf{F}} = \text{CrossAttn}(\mathbf{Q} = \mathbf{F}, \mathbf{K} = \mathbf{T}', \mathbf{V} = \mathbf{T}'). \quad (4)$$

Through this inverse attention mechanism, the face representation is augmented with critical task-specific details, enabling a more robust approach towards facial task unification.

### 3.4 Unified-Head

In Unified-Head, the task tokens are processed to obtain corresponding task predictions. As shown in Fig. 2, the output face tokens  $\hat{\mathbf{F}}$  and task tokens  $\hat{\mathbf{T}}$  are processed through a Task-to-Face Cross-Attention mechanism to obtain final refined features. Then, the output tokens are fed into their corresponding task heads. The task head for landmark detection and head pose estimation is a regression MLP, while the tasks of estimating age, gender, race, visibility, and attributes recognition utilize classification MLPs. For face parsing, we leverage the output  $\hat{\mathbf{F}}$  and process it through an upsampling layer, then perform a cross-product with the face parsing token to obtain a segmentation map. Note, the number of tokens for segmentation corresponds to the total number of classes, and for regression and classification tasks, one token is used per task.

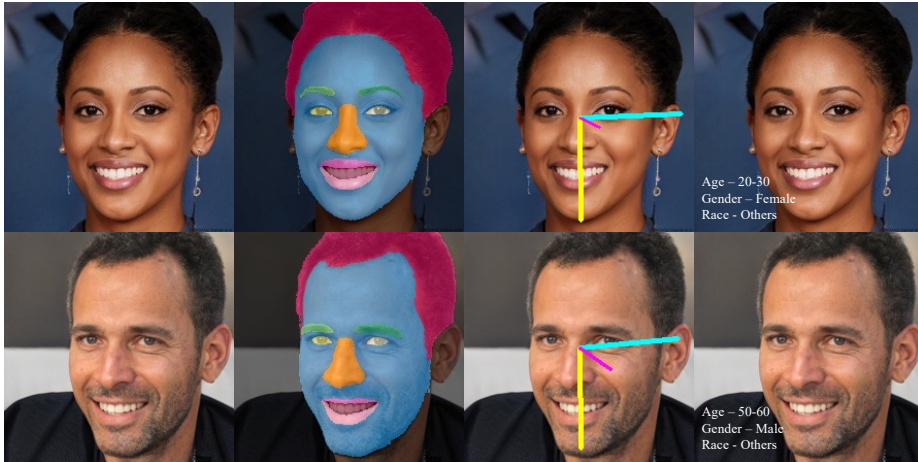


**Fig. 3:** Task-specific inference based on task-tokens on in-the-wild images. In the second column, we query the face parsing token. In the third column, we query the head pose token. In the fourth column, we query the infer age, gender, and race task tokens.

### 3.5 Training and Inference

We aim to train *FaceXFormer* for multiple facial analysis tasks simultaneously, however each task requires distinct and sometimes conflicting pre-processing steps. For instance, landmark detection typically requires keypoint alignment of faces, which contradicts the needs for head pose estimation, as it may eliminate the natural variability of headposes. Due to these reasons, integrating all tasks into a single model poses significant challenges. To address this, *FaceXFormer* incorporates task-specific tokens designed to extract task-specific features from the fused representation. These task tokens compel the backbone to learn a unified representation capable of supporting a broad spectrum of facial analysis tasks. We employ different loss functions for each task and combine them in a joint objective for training. The final loss function is given as:

$$L = \lambda_{seg}L_{seg} + \lambda_{lnd}L_{lnd} + \lambda_{hpe}L_{hpe} + \lambda_{attr}L_{attr} + \lambda_{a/g/r}L_{a/g/r} + \lambda_{vis}L_{vis}, \quad (5)$$

where  $L_{seg}$  is the mean of dice loss [60] and Cross-Entropy (CE) loss for face parsing,  $L_{lnd}$  is wing loss [18] for landmarks estimation,  $L_{hpe}$  is geodesic loss [54] for head pose estimation,  $L_{a/g/r}$  is CE loss for age/gender/race estimation, and  $L_{attr}$  and  $L_{vis}$  are Binary Cross-Entropy with logits loss for attributes recognition and landmarks visibility prediction respectively. During inference, *FaceXFormer* can be prompted for multiple outputs with task-specific tokens. For instance, when prompting for parsing, head pose and age/gender/race, it generates outputs exclusively for those tasks, as illustrated in Figure 3.



## 4 Experiments and Results

### 4.1 Datasets and Metrics

We perform co-training, where the model is simultaneously trained for multiple tasks using a total of ten datasets with task-specific annotations. We conduct intra-dataset and cross-dataset evaluations and present our results on the test sets according to the standard protocol for each task using the following datasets: **Training:** *Face Parsing:* LaPa [41], CelebAMaskHQ [34] *Landmarks Detection:* 300W [53], WFLW [76]; *Head Pose Estimation:* 300W-LP [93], AFLW2000 [94], *Attributes Recognition:* CelebA [42]; *Age/Gender/Race estimation:* UTKFace [85], FairFace [28]; *Landmarks Visibility Prediction:* COFW [5].

**Test (Intra-dataset):** *Face Parsing:* LaPa, CelebAMaskHQ; *Landmarks Detection:* 300W, WFLW; *Attributes Recognition:* CelebA; *Age/Gender/Race Estimation:* UTKFace, FairFace; *Landmarks Visibility Prediction:* COFW.

**Test (Cross-dataset):** *Landmarks Detection:* 300VW [57]; *Head Pose Estimation:* BIWI [16]; *Attributes Recognition:* LFWA [74]; *Age/Gender Estimation:* FFHQ [29]. The evaluation metrics used are F1-score for face parsing, Normalized Mean Error (NME), Failure Rate (FR@10%) and Area Under the Curve (AUC@10%) for landmarks detection, Mean Absolute Error (MAE) for head pose estimation, and accuracy for attributes recognition, age/gender/race estimation and landmarks visibility prediction.

### 4.2 Implementation Details

We train our models using a distributed PyTorch setup on eight A5000 GPUs, each equipped with 24GB of memory. The models’ backbones are initialized with ImageNet pre-trained weights and processes input images at a resolution of  $224 \times 224$ . We employ the AdamW optimizer with a weight decay of  $1e^{-5}$ . All models are trained for 12 epochs with a batch size of 48 on each GPU, and an initial learning rate of  $1e^{-4}$ , which decays by a factor of 10 at the  $6^{th}$  and  $10^{th}$  epochs. For data augmentation, we randomly apply Gaussian blur, grayscale conversion, gamma correction, occlusion, horizontal flipping, and affine transformations, such as rotation, translation and scaling. The number of FaceX decoder  $N$  is set to two. To ensure stable training across tasks when using multiple datasets of varying sample sizes, we equalize the representation of each task’s samples in every batch through upsampling. Additional details on our implementation are provided in the supplementary document.

### 4.3 Main results

In Table 2, we present a comparative analysis of *FaceXFormer* with recent methods across a variety of tasks. A significant highlight of our work is its unique capability to deliver substantial results in all scenarios using a single unified model. *FaceXFormer* achieves state-of-the-art performance in face parsing (@ $224 \times 224$ ) and attributes recognition with a mean F1 of 90.46 over LaPa

Methods	LaPa	CelebAMaskHQ	300W	WFLW	BIWI	CelebA	FairFace		UTKFace	COFW
	F1-score	F1-score	NME	FR <sub>010%</sub>	MAE	Acc.	(Age) Gen {Race}Acc.	(Age) Gen {Race}Acc.	Acc.	
EAGR <sub>473</sub> [65]	91.07	90.84	-	-	-	-	-	-	-	-
AGRNET <sub>473</sub> [64]	92.34	90.67	-	-	-	-	-	-	-	-
DML-CSR <sub>473</sub> [87]	92.38	90.45	-	-	-	-	-	-	-	-
FP-LIIF <sub>256</sub> [56]	90.12	90.09	-	-	-	-	-	-	-	-
Wing [17]	-	-	-	6.00	-	-	-	-	-	-
SBR [14]	-	-	4.10	-	-	-	-	-	-	-
DeCaFa [12]	-	-	3.39	4.84	-	-	-	-	-	-
HRNet [69]	-	-	3.32	4.64	-	-	-	-	-	-
STAR Loss [90]	-	-	2.87	2.32	-	-	-	-	-	-
FDN [83]	-	-	-	-	3.93	-	-	-	-	-
WHENet [89]	-	-	-	-	3.81	-	-	-	-	-
TriNet [7]	-	-	-	-	3.97	-	-	-	-	-
img2pose [2]	-	-	-	-	3.78	-	-	-	-	-
6DRepNet [22]	-	-	-	-	3.47	-	-	-	-	-
TokenHPE [82]	-	-	-	-	3.72	-	-	-	-	-
SSP+SSG [26]	-	-	-	-	-	88.24	-	-	-	-
SSPL [58]	-	-	-	-	-	91.77	-	-	-	-
FairFace [27]	-	-	-	-	-	-	(59.7)/[94.2]/{78.01}	(61.7)/[92.5]/{83.9}	-	-
MiVOLO [32]	-	-	-	-	-	-	(61.07)/[95.73]	-	-	-
SoftCon [23]	-	-	-	-	-	-	-	{87.00}	-	-
EnD [63]	-	-	-	-	-	-	-	{88.40}	-	-
ProS [13]	92.00	-	3.27	-	-	91.88	-	-	-	-
FaRL [88]	91.62	90.34	3.35	5.72	-	91.39	(61.78)/[95.65]	-	-	-
HyperFace [51]	-	-	3.62	6.09	3.46	-	[94.26]	[95.52]	-	88.91
AllinOne [52]	-	-	4.52	15.45	5.64	-	(54.18)/[88.22]	(61.48)/[93.70]	-	84.11
<b>FaceXFormer</b>	91.10	89.83	3.53	4.56	3.65	91.79	(59.38)/[95.20]/{77.91}	(63.93)/[95.69]/{87.45}	-	90.16

**Table 2:** Comparison with specialized models and existing multi-task networks

and CelebAMaskHQ, and a mean accuracy of 91.79 on CelebA. We observe that the performance on age/gender/race estimation is on par with some specialized bias-mitigation methods, showing that it exhibits minimal bias on these factors, even when trained on a small number of data points. This aspect is further explored in the ethical considerations section. *FaceXFormer* demonstrates competitive performance at par with leading methods like STAR Loss [90] and TokenHPE [82] for landmarks detection and head pose estimation respectively. The performance discrepancy in landmarks detection is mainly because we don't employ additional heatmaps during training, which is the recent trend in landmarks detection literature. Similarly, current works utilize different head pose representations such as rotation matrix and 6D representation to improve performance. We avoid using auxiliary information and advanced representations as our goal is not to specialize in a single task, but to learn a unified representation suitable for a wide spectrum of tasks.

We also compare our work with recent models that aim at unification. ProS [13] and FaRL [88] are pretraining methods for face tasks aimed at learning a strong encoder that generates generalized feature representations. This work is tangential to HyperFace [52] and AllinOne [52], which are more similar to our proposal, i.e., learning of a unified decoder. We observe that *FaceXFormer* outperforms other unified model baselines across multiple benchmarks. However, HyperFace performs better in head pose estimation. We observe that different tasks complement each other and boost each other's performance, as can be seen in the case of HyperFace. HyperFace is jointly trained for landmarks detection and head pose

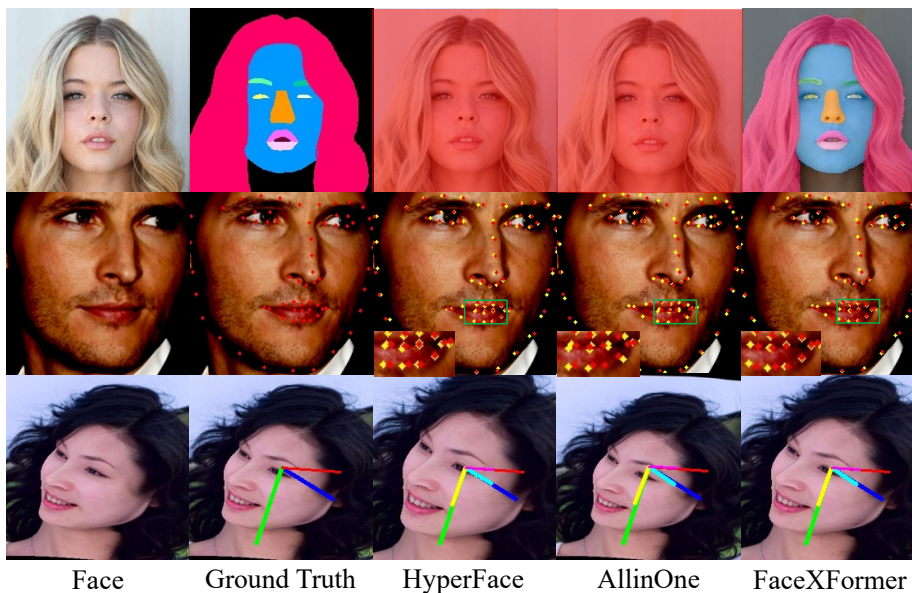


Fig. 4: Qualitative comparison of *FaceXFormer* against other multi-task models

estimation, both of which are regression-based tasks that mutually enhance their performance. We observe a similar performance increase when *FaceXFormer* is trained exclusively on regression-based tasks. This enhancement is primarily because the model has learned regression-specific feature representations, which are optimized for these tasks. However, when these tasks are combined with others that do not share the same feature requirements, we notice a decrement in performance. We further explore the task synergy of *FaceXFormer* in the ablation section of our work.

In our work, we simultaneously train for eight heterogeneous tasks, presenting a formidable challenge compared to previous works. This challenge arises primarily because these tasks require task-specific features and pre-processing steps, given the tasks are so distinct and diverse. This ability to effectively handle a multitude of facial analysis tasks, despite the small performance gaps noted, reinforces our assertion that *FaceXFormer* is a unified versatile model suitable for diverse facial analysis tasks.

#### 4.4 Qualitative results

In Figure 4, we present the qualitative results of *FaceXFormer* for a selected subset of tasks and compare it against other baselines. Specifically, in the second row, we highlight our superior performance in landmarks detection. In the first row, we display the face parsing results, demonstrating tasks beyond what HyperFace and AllinOne can perform. As discussed in Section 3, *FaceXFormer* can

be prompted with task-specific tokens during inference to obtain multiple predictions. We prompt two random in-the-wild faces for face parsing, head pose, age, gender and race estimation and show the results in Figure 3. This demonstrates *FaceXFormer’s* robust performance in in-the-wild scenarios.

#### 4.5 Ablation Study

**Table 3:** Ablation analysis for multi-task synergy between segmentation, regression and classification

Seg	Reg	Cls	Seg	Reg	Cls
			F1	NME	Acc.
✓			89.64	-	-
	✓		-	3.84	-
		✓	-	-	82.53
✓	✓	✓	90.46	3.99	82.68

**Table 4:** Performance analysis with different backbones and different backbone size

Backbone	Seg	Reg	Cls
	F1	NME	Acc.
ResNet101	89.63	4.16	82.15
ConvNext	90.77	3.92	82.60
Swin/T	89.91	4.1	82.43
Swin/S	90.18	3.90	82.38
Swin/B	90.46	3.99	82.68

In this section, we discuss how different tasks synergize to boost performance and explore the impact of various backbones and their sizes on performance. Additionally, we highlight the importance of multi-scale feature fusion.

#### 4.6 Task Synergy

We train *FaceXFormer* on a subset of tasks, categorizing them into three categories: Segmentation (Seg), Regression (Reg), and Classification (Cls). Segmentation includes face parsing; regression encompasses landmarks detection and head pose estimation; and classification covers attributes recognition, age/gender/race estimation, and landmarks visibility prediction. From Table 3, we can see that segmentation and classification performance is better when trained jointly with other tasks. However, we observe a small drop in performance when tasks are trained jointly with the regression category. We attribute this to the fact that different tasks require different kinds of representations for prediction. Segmentation demands fine-grained feature representations; attributes recognition and other classification tasks require semantic information, while regression-based tasks necessitate a blend of high-level and finer features. Our proposed *FaceXFormer* addresses this challenge by using fused feature representations and treating multiple tasks as tokens, thereby making joint training across multiple tasks effective.

#### 4.7 Effect of different backbone and different size for *FaceXformer*

In Table 4, we conducted experiments to analyze the effect of different backbones and their sizes on *FaceXformer*. ConvNext leads in segmentation and regression with an F1 score of 90.77% and an NME of 3.92, but is closely followed by Swin Transformer variants, which exhibit competitive performance and superior scalability. Conversely, ResNet101 shows the lowest metrics, such as an F1 score of 89.63% and an NME of 4.16, indicating its limitations in handling larger, more complex datasets and its smaller receptive field compared to Swin Transformers. The choice of Swin Transformer over ConvNext for *FaceXformer* is based on its enhanced scaling capabilities and superior global contextual understanding, which are crucial for facial analysis tasks, despite its slightly lower scores in certain metrics. This decision underscores the importance of fitting the backbone to the model’s architecture to improve overall task synergy and performance.

## 5 Discussions

In this section, we discuss the broader impact of our work. Additionally, we talk about the ethical considerations and limitations of *FaceXFormer*.

### 5.1 Broader Impact

The world is moving towards transformers because of its potential to model large amounts of data [3, 4, 30]. Presently, the face community lacks large-scale annotated datasets to train foundational models capable of performing a wide spectrum of facial tasks. The largest clean dataset, WebFace42M [96], lacks annotations for face parsing, landmarks detection and attributes recognition. *FaceXFormer* can be used as an annotator for large-scale data, and can be continually improved through successive rounds of annotation and fine-tuning. We aim to propel the face community towards developing foundation models that cater to a variety of facial tasks. Additionally, *FaceXFormer* is a lightweight model that provides real-time output based on task-specific queries and can be appended with existing facial detection systems to provide additional information. It can also serve as a valuable tool in surveillance, and provide auxiliary information for subject analysis and image retrieval.

### 5.2 Ethical considerations

In our work, we utilize a total of 14 datasets for training and evaluation. We obtain these datasets following the procedures stated on their respective pages and signed the license agreements if and when necessary. As we train our models on multiple datasets designed for different tasks, the representation of subjects across different age groups, genders, and races is not equal. This imbalance may introduce bias in the model. Therefore, we provide an analysis using the FairFace [27] dataset, which is balanced in terms of age, gender and race. We

follow [49] and define the "Non-white" group to include multiple racial categories: "Black", "Indian", "East Asian", "Southeast Asian", "Middle Eastern" and "Latino". As can be seen from Table 5, *FaceXFormer* shows the smallest performance discrepancy across different racial groups and exhibits minimal bias compared to other models, despite being trained on fewer data points. This can be attributed to race estimation being of the tasks in co-training.

	Model	Data Points	White	Non-white	Average	Discrepancy
Age	FairFace	100K	60.05	60.63	60.52	0.58
	CLIP	400M	62.25	61.95	62.00	-0.30
	FaRL	20M	61.49	61.84	61.78	0.35
	FaceXFormer	400K	58.94	59.44	59.34	0.50
Gender	FairFace	100K	94.15	94.41	94.36	0.26
	CLIP	400M	94.87	95.78	95.61	0.91
	FaRL	20M	95.16	95.77	95.65	0.61
	FaceXFormer	400K	95.34	95.19	95.22	-0.09

**Table 5:** Age and gender accuracy w.r.t two race groups on FairFace

### 5.3 Limitations

We acknowledge the shortcomings of the proposed *FaceXFormer* in not achieving state-of-the-art performance in certain tasks, such as landmarks detection and head pose estimation. This is primarily because the SOTA models for these tasks utilize auxiliary heat-map based loss and advanced representations, respectively. Nevertheless, *FaceXFormer* uniquely handles up to eight different heterogeneous tasks within a single model and offers competitive performance across these tasks in real-time, enhancing its suitability for deployment. Additionally, while it supports tokens for various tasks, it is not yet interactive and lacks full promptability. Our future work will focus on developing an interactive foundational model capable of handling multiple tasks.

## 6 Conclusion

In conclusion, the *FaceXformer* introduces a novel end-to-end unified model that efficiently handles a comprehensive range of facial analysis tasks. By adopting a transformer-based encoder-decoder architecture and treating each task as a learnable token, our approach successfully integrates multiple tasks within a single framework. The proposed parameter-efficient decoder, FaceX, enhances the model's ability to learn robust and generalized face representations across diverse tasks. Our comprehensive experiments show how segmentation, regression, and classification facial analysis tasks improve each other. Additionally, training on multiple datasets leads to better representation learning. In conclusion, we demonstrate that facial tasks can be treated as tokens, leading to the unification of tasks; following this, we hope our work provides a foundation for developing models capable of performing multiple facial analysis tasks.

## Acknowledgements

This research is based upon work supported in part by the Office of the Director of National Intelligence (ODNI), Intelligence Advanced Research Projects Activity (IARPA), via [2022-21102100005]. The views and conclusions contained herein are those of the authors and should not be interpreted as necessarily representing the official policies, either expressed or implied, of ODNI, IARPA, or the U.S. Government. The US Government is authorized to reproduce and distribute reprints for governmental purposes notwithstanding any copyright annotation therein.

## References

1. Abirami, B., Subashini, T., Mahavaishnavi, V.: Gender and age prediction from real time facial images using cnn. *Materials Today: Proceedings* **33**, 4708–4712 (2020)
2. Albiero, V., Chen, X., Yin, X., Pang, G., Hassner, T.: img2pose: Face alignment and detection via 6dof, face pose estimation. In: *Proceedings of the IEEE/CVF conference on computer vision and pattern recognition*. pp. 7617–7627 (2021)
3. Brooks, T., Peebles, B., Holmes, C., DePue, W., Guo, Y., Jing, L., Schnurr, D., Taylor, J., Luhman, T., Luhman, E., Ng, C., Wang, R., Ramesh, A.: Video generation models as world simulators (2024), <https://openai.com/research/video-generation-models-as-world-simulators>
4. Brown, T., Mann, B., Ryder, N., Subbiah, M., Kaplan, J.D., Dhariwal, P., Neelakantan, A., Shyam, P., Sastry, G., Askell, A., et al.: Language models are few-shot learners. *Advances in neural information processing systems* **33**, 1877–1901 (2020)
5. Burgos-Artizzu, X.P., Perona, P., Dollár, P.: Robust face landmark estimation under occlusion. In: *Proceedings of the IEEE international conference on computer vision*. pp. 1513–1520 (2013)
6. Cao, W., Mirjalili, V., Raschka, S.: Rank consistent ordinal regression for neural networks with application to age estimation. *Pattern Recognition Letters* **140**, 325–331 (2020)
7. Cao, Z., Chu, Z., Liu, D., Chen, Y.: A vector-based representation to enhance head pose estimation. In: *Proceedings of the IEEE/CVF Winter Conference on applications of computer vision*. pp. 1188–1197 (2021)
8. Carion, N., Massa, F., Synnaeve, G., Usunier, N., Kirillov, A., Zagoruyko, S.: End-to-end object detection with transformers. In: *European conference on computer vision*. pp. 213–229. Springer (2020)
9. Chen, L.C., Yang, Y., Wang, J., Xu, W., Yuille, A.L.: Attention to scale: Scale-aware semantic image segmentation. In: *Proceedings of the IEEE conference on computer vision and pattern recognition*. pp. 3640–3649 (2016)
10. Cobo, A., Valle, R., Buenaposada, J.M., Baumela, L.: On the representation and methodology for wide and short range head pose estimation. *Pattern Recognition* **149**, 110263 (2024)
11. Cui, K., Wu, R., Zhan, F., Lu, S.: Face transformer: Towards high fidelity and accurate face swapping. In: *Proceedings of the IEEE/CVF Conference on Computer Vision and Pattern Recognition*. pp. 668–677 (2023)

12. Dapogny, A., Bailly, K., Cord, M.: Decafa: Deep convolutional cascade for face alignment in the wild. In: Proceedings of the IEEE/CVF International Conference on Computer Vision. pp. 6893–6901 (2019)
13. Di, X., Zheng, Y., Liu, X., Cheng, Y.: Pros: Facial omni-representation learning via prototype-based self-distillation. In: Proceedings of the IEEE/CVF Winter Conference on Applications of Computer Vision. pp. 6087–6098 (2024)
14. Dong, X., Yu, S.I., Weng, X., Wei, S.E., Yang, Y., Sheikh, Y.: Supervision-by-registration: An unsupervised approach to improve the precision of facial landmark detectors. In: Proceedings of the IEEE Conference on Computer Vision and Pattern Recognition. pp. 360–368 (2018)
15. Dosovitskiy, A., Beyer, L., Kolesnikov, A., Weissenborn, D., Zhai, X., Unterthiner, T., Dehghani, M., Minderer, M., Heigold, G., Gelly, S., et al.: An image is worth 16x16 words: Transformers for image recognition at scale. arXiv preprint arXiv:2010.11929 (2020)
16. Fanelli, G., Dantone, M., Gall, J., Fossati, A., Van Gool, L.: Random forests for real time 3d face analysis. *International journal of computer vision* **101**, 437–458 (2013)
17. Feng, Z.H., Kittler, J., Awais, M., Huber, P., Wu, X.J.: Wing loss for robust facial landmark localisation with convolutional neural networks. In: Proceedings of the IEEE Conference on Computer Vision and Pattern Recognition (CVPR) (June 2018)
18. Feng, Z.H., Kittler, J., Awais, M., Huber, P., Wu, X.J.: Wing loss for robust facial landmark localisation with convolutional neural networks. In: Proceedings of the IEEE conference on computer vision and pattern recognition. pp. 2235–2245 (2018)
19. Ghaleb, A.E.K., Boumaiza, S., Amara, N.E.B.: Demographic face profiling based on age, gender and race. In: 2020 5th International Conference on Advanced Technologies for Signal and Image Processing (ATSIP). pp. 1–6. IEEE (2020)
20. Girshick, R., Donahue, J., Darrell, T., Malik, J.: Rich feature hierarchies for accurate object detection and semantic segmentation. In: Proceedings of the IEEE conference on computer vision and pattern recognition. pp. 580–587 (2014)
21. Han, H., Jain, A.K., Wang, F., Shan, S., Chen, X.: Heterogeneous face attribute estimation: A deep multi-task learning approach. *IEEE transactions on pattern analysis and machine intelligence* **40**(11), 2597–2609 (2017)
22. Hempel, T., Abdelrahman, A.A., Al-Hamadi, A.: 6d rotation representation for unconstrained head pose estimation. In: 2022 IEEE International Conference on Image Processing (ICIP). pp. 2496–2500. IEEE (2022)
23. Hong, Y., Yang, E.: Unbiased classification through bias-contrastive and bias-balanced learning. *Advances in Neural Information Processing Systems* **34**, 26449–26461 (2021)
24. Hsieh, H.L., Hsu, W., Chen, Y.Y.: Multi-task learning for face identification and attribute estimation. In: 2017 IEEE International Conference on Acoustics, Speech and Signal Processing (ICASSP). pp. 2981–2985 (2017). <https://doi.org/10.1109/ICASSP.2017.7952703>
25. Jackson, A.S., Valstar, M., Tzimiropoulos, G.: A cnn cascade for landmark guided semantic part segmentation. In: Computer Vision–ECCV 2016 Workshops: Amsterdam, The Netherlands, October 8–10 and 15–16, 2016, Proceedings, Part III 14. pp. 143–155. Springer (2016)
26. Kalayeh, M.M., Gong, B., Shah, M.: Improving facial attribute prediction using semantic segmentation. In: Proceedings of the IEEE Conference on Computer Vision and Pattern Recognition. pp. 6942–6950 (2017)



27. Karkkainen, K., Joo, J.: Fairface: Face attribute dataset for balanced race, gender, and age for bias measurement and mitigation. In: Proceedings of the IEEE/CVF winter conference on applications of computer vision. pp. 1548–1558 (2021)
28. Karkkainen, K., Joo, J.: Fairface: Face attribute dataset for balanced race, gender, and age for bias measurement and mitigation. In: Proceedings of the IEEE/CVF Winter Conference on Applications of Computer Vision. pp. 1548–1558 (2021)
29. Karras, T., Laine, S., Aila, T.: A style-based generator architecture for generative adversarial networks. In: Proceedings of the IEEE/CVF conference on computer vision and pattern recognition. pp. 4401–4410 (2019)
30. Kirillov, A., Mintun, E., Ravi, N., Mao, H., Rolland, C., Gustafson, L., Xiao, T., Whitehead, S., Berg, A.C., Lo, W.Y., et al.: Segment anything. arXiv preprint arXiv:2304.02643 (2023)
31. Kumar, A., Marks, T.K., Mou, W., Wang, Y., Jones, M., Cherian, A., Koike-Akino, T., Liu, X., Feng, C.: Luvli face alignment: Estimating landmarks’ location, uncertainty, and visibility likelihood. In: Proceedings of the IEEE/CVF Conference on Computer Vision and Pattern Recognition. pp. 8236–8246 (2020)
32. Kuprashevich, M., Tolstykh, I.: Mivolo: Multi-input transformer for age and gender estimation. arXiv preprint arXiv:2307.04616 (2023)
33. Lan, X., Hu, Q., Chen, Q., Xue, J., Cheng, J.: Hih: Towards more accurate face alignment via heatmap in heatmap. arXiv preprint arXiv:2104.03100 (2021)
34. Lee, C.H., Liu, Z., Wu, L., Luo, P.: Maskgan: Towards diverse and interactive facial image manipulation. In: IEEE Conference on Computer Vision and Pattern Recognition (CVPR) (2020)
35. Levi, G., Hassner, T.: Age and gender classification using convolutional neural networks. In: Proceedings of the IEEE conference on computer vision and pattern recognition workshops. pp. 34–42 (2015)
36. Li, J., Jin, H., Liao, S., Shao, L., Heng, P.A.: Repformer: Refinement pyramid transformer for robust facial landmark detection. arXiv preprint arXiv:2207.03917 (2022)
37. Li, W., Huang, X., Lu, J., Feng, J., Zhou, J.: Learning probabilistic ordinal embeddings for uncertainty-aware regression. In: Proceedings of the IEEE/CVF conference on computer vision and pattern recognition. pp. 13896–13905 (2021)
38. Li, X., Yuan, H., Li, W., Ding, H., Wu, S., Zhang, W., Li, Y., Chen, K., Loy, C.C.: Omg-seg: Is one model good enough for all segmentation? arXiv preprint arXiv:2401.10229 (2024)
39. Lin, C., Zhu, B., Wang, Q., Liao, R., Qian, C., Lu, J., Zhou, J.: Structure-coherent deep feature learning for robust face alignment. IEEE Transactions on Image Processing **30**, 5313–5326 (2021)
40. Lin, J., Yang, H., Chen, D., Zeng, M., Wen, F., Yuan, L.: Face parsing with roi tanh-warping. In: Proceedings of the IEEE/CVF Conference on Computer Vision and Pattern Recognition. pp. 5654–5663 (2019)
41. Liu, Y., Shi, H., Shen, H., Si, Y., Wang, X., Mei, T.: A new dataset and boundary-attention semantic segmentation for face parsing. In: AAAI. pp. 11637–11644 (2020)
42. Liu, Z., Luo, P., Wang, X., Tang, X.: Deep learning face attributes in the wild. In: Proceedings of International Conference on Computer Vision (ICCV) (December 2015)
43. Mi, C., Yuan, B., Ma, P., Guo, Y., Qi, L., Wang, F., Wu, W., Wang, L.: Visibility prediction based on landmark detection in foggy weather. In: 2020 International Conference on Robots & Intelligent System (ICRIS). pp. 134–137 (2020). <https://doi.org/10.1109/ICRIS52159.2020.00041>

44. Micaelli, P., Vahdat, A., Yin, H., Kautz, J., Molchanov, P.: Recurrence without recurrence: Stable video landmark detection with deep equilibrium models. In: Proceedings of the IEEE/CVF Conference on Computer Vision and Pattern Recognition. pp. 22814–22825 (2023)
45. Ming, Z., Xia, J., Luqman, M.M., Burie, J.C., Zhao, K.: Dynamic multi-task learning for face recognition with facial expression. arXiv preprint arXiv:1911.03281 (2019)
46. Miyato, T., Maeda, S.i., Koyama, M., Ishii, S.: Virtual adversarial training: a regularization method for supervised and semi-supervised learning. *IEEE transactions on pattern analysis and machine intelligence* **41**(8), 1979–1993 (2018)
47. Murphy-Chutorian, E., Doshi, A., Trivedi, M.M.: Head pose estimation for driver assistance systems: A robust algorithm and experimental evaluation. In: 2007 IEEE intelligent transportation systems conference. pp. 709–714. IEEE (2007)
48. Noroozi, M., Favaro, P.: Unsupervised learning of visual representations by solving jigsaw puzzles. In: European conference on computer vision. pp. 69–84. Springer (2016)
49. Radford, A., Kim, J.W., Hallacy, C., Ramesh, A., Goh, G., Agarwal, S., Sastry, G., Askell, A., Mishkin, P., Clark, J., et al.: Learning transferable visual models from natural language supervision. In: International conference on machine learning. pp. 8748–8763. PMLR (2021)
50. Ramesh, A., Pavlov, M., Goh, G., Gray, S., Voss, C., Radford, A., Chen, M., Sutskever, I.: Zero-shot text-to-image generation. In: International Conference on Machine Learning. pp. 8821–8831. PMLR (2021)
51. Ranjan, R., Patel, V.M., Chellappa, R.: Hyperface: A deep multi-task learning framework for face detection, landmark localization, pose estimation, and gender recognition. *IEEE transactions on pattern analysis and machine intelligence* **41**(1), 121–135 (2017)
52. Ranjan, R., Sankaranarayanan, S., Castillo, C.D., Chellappa, R.: An all-in-one convolutional neural network for face analysis. In: 2017 12th IEEE international conference on automatic face & gesture recognition (FG 2017). pp. 17–24. IEEE (2017)
53. Sagonas, C., Tzimiropoulos, G., Zafeiriou, S., Pantic, M.: 300 faces in-the-wild challenge: The first facial landmark localization challenge. In: Proceedings of the IEEE international conference on computer vision workshops. pp. 397–403 (2013)
54. Salehi, S.S.M., Khan, S., Erdogmus, D., Gholipour, A.: Real-time deep pose estimation with geodesic loss for image-to-template rigid registration. *IEEE transactions on medical imaging* **38**(2), 470–481 (2018)
55. Van de Sande, K.E., Uijlings, J.R., Gevers, T., Smeulders, A.W.: Segmentation as selective search for object recognition. In: 2011 international conference on computer vision. pp. 1879–1886. IEEE (2011)
56. Sarkar, M., Hemani, M., Jain, R., Krishnamurthy, B., et al.: Parameter efficient local implicit image function network for face segmentation. In: Proceedings of the IEEE/CVF Conference on Computer Vision and Pattern Recognition. pp. 20970–20980 (2023)
57. Shen, J., Zafeiriou, S., Chrysos, G.G., Kossaiji, J., Tzimiropoulos, G., Pantic, M.: The first facial landmark tracking in-the-wild challenge: Benchmark and results. In: Proceedings of the IEEE international conference on computer vision workshops. pp. 50–58 (2015)
58. Shu, Y., Yan, Y., Chen, S., Xue, J.H., Shen, C., Wang, H.: Learning spatial-semantic relationship for facial attribute recognition with limited labeled data.

- In: Proceedings of the IEEE/CVF Conference on Computer Vision and Pattern Recognition. pp. 11916–11925 (2021)
59. Strazdas, D., Hintz, J., Al-Hamadi, A.: Robo-hud: Interaction concept for contactless operation of industrial cobotic systems. *Applied Sciences* **11**(12), 5366 (2021)
  60. Sudre, C.H., Li, W., Vercauteren, T., Ourselin, S., Jorge Cardoso, M.: Generalised dice overlap as a deep learning loss function for highly unbalanced segmentations. In: Deep Learning in Medical Image Analysis and Multimodal Learning for Clinical Decision Support: Third International Workshop, DLMIA 2017, and 7th International Workshop, ML-CDS 2017, Held in Conjunction with MICCAI 2017, Québec City, QC, Canada, September 14, Proceedings 3. pp. 240–248. Springer (2017)
  61. Sun, Y., Chen, Y., Wang, X., Tang, X.: Deep learning face representation by joint identification-verification. *Advances in neural information processing systems* **27** (2014)
  62. Taigman, Y., Yang, M., Ranzato, M., Wolf, L.: Deepface: Closing the gap to human-level performance in face verification. In: Proceedings of the IEEE conference on computer vision and pattern recognition. pp. 1701–1708 (2014)
  63. Tartaglione, E., Barbano, C.A., Grangetto, M.: End: Entangling and disentangling deep representations for bias correction. In: Proceedings of the IEEE/CVF conference on computer vision and pattern recognition. pp. 13508–13517 (2021)
  64. Te, G., Hu, W., Liu, Y., Shi, H., Mei, T.: Agrnet: Adaptive graph representation learning and reasoning for face parsing. *IEEE Transactions on Image Processing* **30**, 8236–8250 (2021)
  65. Te, G., Liu, Y., Hu, W., Shi, H., Mei, T.: Edge-aware graph representation learning and reasoning for face parsing. In: Computer Vision–ECCV 2020: 16th European Conference, Glasgow, UK, August 23–28, 2020, Proceedings, Part XII 16. pp. 258–274. Springer (2020)
  66. Touvron, H., Lavril, T., Izacard, G., Martinet, X., Lachaux, M.A., Lacroix, T., Rozière, B., Goyal, N., Hambro, E., Azhar, F., et al.: Llama: Open and efficient foundation language models. *arXiv preprint arXiv:2302.13971* (2023)
  67. Valle, R., Buenaposada, J.M., Baumela, L.: Multi-task head pose estimation in-the-wild. *IEEE Transactions on Pattern Analysis and Machine Intelligence* **43**(8), 2874–2881 (2020)
  68. Vaswani, A., Shazeer, N., Parmar, N., Uszkoreit, J., Jones, L., Gomez, A.N., Kaiser, Ł., Polosukhin, I.: Attention is all you need. *Advances in neural information processing systems* **30** (2017)
  69. Wang, J., Sun, K., Cheng, T., Jiang, B., Deng, C., Zhao, Y., Liu, D., Mu, Y., Tan, M., Wang, X., et al.: Deep high-resolution representation learning for visual recognition. *IEEE transactions on pattern analysis and machine intelligence* **43**(10), 3349–3364 (2020)
  70. Wang, J., Chen, D., Wu, Z., Luo, C., Zhou, L., Zhao, Y., Xie, Y., Liu, C., Jiang, Y.G., Yuan, L.: Omnivl: One foundation model for image-language and video-language tasks. *Advances in neural information processing systems* **35**, 5696–5710 (2022)
  71. Wang, Q., Chang, Y.Y., Cai, R., Li, Z., Hariharan, B., Holynski, A., Snavely, N.: Tracking everything everywhere all at once. *arXiv preprint arXiv:2306.05422* (2023)
  72. Wang, Z., Li, Y., Chen, X., Lim, S.N., Torralla, A., Zhao, H., Wang, S.: Detecting everything in the open world: Towards universal object detection. In: Proceedings of the IEEE/CVF Conference on Computer Vision and Pattern Recognition. pp. 11433–11443 (2023)

73. Wei, Z., Sun, Y., Wang, J., Lai, H., Liu, S.: Learning adaptive receptive fields for deep image parsing network. In: Proceedings of the IEEE conference on computer vision and pattern recognition. pp. 2434–2442 (2017)
74. Wolf, L., Hassner, T., Taigman, Y.: Effective unconstrained face recognition by combining multiple descriptors and learned background statistics. *IEEE transactions on pattern analysis and machine intelligence* **33**(10), 1978–1990 (2010)
75. Wood, E., Baltrušaitis, T., Hewitt, C., Johnson, M., Shen, J., Milosavljević, N., Wilde, D., Garbin, S., Sharp, T., Stojiljković, I., et al.: 3d face reconstruction with dense landmarks. In: European Conference on Computer Vision. pp. 160–177. Springer (2022)
76. Wu, W., Qian, C., Yang, S., Wang, Q., Cai, Y., Zhou, Q.: Look at boundary: A boundary-aware face alignment algorithm. In: CVPR (June 2018)
77. Xie, E., Wang, W., Yu, Z., Anandkumar, A., Alvarez, J.M., Luo, P.: Segformer: Simple and efficient design for semantic segmentation with transformers. *Advances in Neural Information Processing Systems* **34**, 12077–12090 (2021)
78. Yan, X., Yang, J., Sohn, K., Lee, H.: Attribute2image: Conditional image generation from visual attributes. In: Computer Vision–ECCV 2016: 14th European Conference, Amsterdam, The Netherlands, October 11–14, 2016, Proceedings, Part IV 14. pp. 776–791. Springer (2016)
79. Yin, X., Huang, D., Fu, Z., Wang, Y., Chen, L.: Segmentation-reconstruction-guided facial image de-occlusion. In: 2023 IEEE 17th International Conference on Automatic Face and Gesture Recognition (FG). pp. 1–8. IEEE (2023)
80. Yuan, L., Chen, D., Chen, Y.L., Codella, N., Dai, X., Gao, J., Hu, H., Huang, X., Li, B., Li, C., et al.: Florence: A new foundation model for computer vision. *arXiv preprint arXiv:2111.11432* (2021)
81. Zaeemzadeh, A., Ghadar, S., Faieta, B., Lin, Z., Rahnavard, N., Shah, M., Kalarot, R.: Face image retrieval with attribute manipulation. In: Proceedings of the IEEE/CVF International Conference on Computer Vision. pp. 12116–12125 (2021)
82. Zhang, C., Liu, H., Deng, Y., Xie, B., Li, Y.: Tokenhpe: Learning orientation tokens for efficient head pose estimation via transformers. In: Proceedings of the IEEE/CVF Conference on Computer Vision and Pattern Recognition. pp. 8897–8906 (2023)
83. Zhang, H., Wang, M., Liu, Y., Yuan, Y.: Fdn: Feature decoupling network for head pose estimation. In: Proceedings of the AAAI conference on artificial intelligence. vol. 34, pp. 12789–12796 (2020)
84. Zhang, Z., Luo, P., Loy, C.C., Tang, X.: Facial landmark detection by deep multi-task learning. In: Computer Vision–ECCV 2014: 13th European Conference, Zurich, Switzerland, September 6–12, 2014, Proceedings, Part VI 13. pp. 94–108. Springer (2014)
85. Zhang, Z., Song, Y., Qi, H.: Age progression/regression by conditional adversarial autoencoder. In: Proceedings of the IEEE conference on computer vision and pattern recognition. pp. 5810–5818 (2017)
86. Zhao, R., Liu, T., Xiao, J., Lun, D.P., Lam, K.M.: Deep multi-task learning for facial expression recognition and synthesis based on selective feature sharing. In: 2020 25th International Conference on Pattern Recognition (ICPR). pp. 4412–4419. IEEE (2021)
87. Zheng, Q., Deng, J., Zhu, Z., Li, Y., Zafeiriou, S.: Decoupled multi-task learning with cyclical self-regulation for face parsing. In: Proceedings of the IEEE/CVF Conference on Computer Vision and Pattern Recognition. pp. 4156–4165 (2022)

88. Zheng, Y., Yang, H., Zhang, T., Bao, J., Chen, D., Huang, Y., Yuan, L., Chen, D., Zeng, M., Wen, F.: General facial representation learning in a visual-linguistic manner. In: Proceedings of the IEEE/CVF Conference on Computer Vision and Pattern Recognition. pp. 18697–18709 (2022)
89. Zhou, Y., Gregson, J.: Whenet: Real-time fine-grained estimation for wide range head pose. arXiv preprint arXiv:2005.10353 (2020)
90. Zhou, Z., Li, H., Liu, H., Wang, N., Yu, G., Ji, R.: Star loss: Reducing semantic ambiguity in facial landmark detection. In: Proceedings of the IEEE/CVF Conference on Computer Vision and Pattern Recognition. pp. 15475–15484 (2023)
91. Zhu, J., Lai, S., Chen, X., Wang, D., Lu, H.: Visual prompt multi-modal tracking. In: Proceedings of the IEEE/CVF Conference on Computer Vision and Pattern Recognition. pp. 9516–9526 (2023)
92. Zhu, P., Abdal, R., Qin, Y., Wonka, P.: Sean: Image synthesis with semantic region-adaptive normalization. In: Proceedings of the IEEE/CVF Conference on Computer Vision and Pattern Recognition. pp. 5104–5113 (2020)
93. Zhu, X., Lei, Z., Liu, X., Shi, H., Li, S.Z.: Face alignment across large poses: A 3d solution. In: Proceedings of the IEEE conference on computer vision and pattern recognition. pp. 146–155 (2016)
94. Zhu, X., Lei, Z., Yan, J., Yi, D., Li, S.Z.: High-fidelity pose and expression normalization for face recognition in the wild. In: Proceedings of the IEEE conference on computer vision and pattern recognition. pp. 787–796 (2015)
95. Zhu, X., Su, W., Lu, L., Li, B., Wang, X., Dai, J.: Deformable detr: Deformable transformers for end-to-end object detection. arXiv preprint arXiv:2010.04159 (2020)
96. Zhu, Z., Huang, G., Deng, J., Ye, Y., Huang, J., Chen, X., Zhu, J., Yang, T., Lu, J., Du, D., et al.: Webface260m: A benchmark unveiling the power of million-scale deep face recognition. In: Proceedings of the IEEE/CVF Conference on Computer Vision and Pattern Recognition. pp. 10492–10502 (2021)
97. Zhuang, N., Yan, Y., Chen, S., Wang, H.: Multi-task learning of cascaded cnn for facial attribute classification. In: 2018 24th International Conference on Pattern Recognition (ICPR). pp. 2069–2074. IEEE (2018)
98. Zou, X., Yang, J., Zhang, H., Li, F., Li, L., Wang, J., Wang, L., Gao, J., Lee, Y.J.: Segment everything everywhere all at once. *Advances in Neural Information Processing Systems* **36** (2024)

## A Overview

As part of the supplementary material, we present the following as an extension to the ones shown in the paper:

- Cross-dataset Evaluation (Section B)
- Parameter and FPS Analysis (Section C)
- In-the-wild Visualization (Section D)
- Additional Results (Section E)
- Additional Training details (Section F)

## B Cross-Dataset Evaluation

Method	300VW	LFWA	FFHQ(Age)	FFHQ(Gender)
	NME	Acc.	Acc.	Acc.
HyperFace [51]	8.50	-	-	91.90
AllinOne [52]	7.28	-	34.88	80.83
<b><i>FaceXFormer</i></b>	9.83	72.23	46.60	94.92

**Table 6:** Cross Dataset evaluation of *FaceXFormer* in comparison to existing multi-task models

We conduct additional cross-dataset experiments to demonstrate the effectiveness of *FaceXFormer* in scenarios closely resembling real life, where face images are previously unseen, unconstrained, and characterized by significant variability in background, lighting, pose, and other factors. From Table 6, it is evident that *FaceXFormer* surpasses existing multi-task baselines in classification tasks. However, its effectiveness in landmark detection under in-the-wild scenarios is only moderate. The paper provides an explanation for this behavior, which we reiterate here: HyperFace [51] and AllInOne [52] are primarily trained on regression-based tasks, which boosts their performance on individual regression tasks. Consequently, they might outperform *FaceXFormer* in landmark detection but fall short in other tasks that only *FaceXFormer* can handle. The cross-dataset results echoes our rationale presented in the paper: the need for a unified facial analysis model capable of performing multiple tasks on in-the-wild, unconstrained faces, particularly for real-life applications. *FaceXFormer* addresses this gap and demonstrates competitive performance across various tasks.

## C Parameter and FPS Analysis

The parameter and FPS analysis for different backbones in the *FaceXformer* framework provides insightful trends regarding computational efficiency and per-

Model	Params	GFLOPs	FPS	B4FPS
Swin-B	91.98	17.98	39.89	150.25
Swin-B (seg)	91.06	17.93	41.09	156.19
Swin-B (reg)	91.01	17.54	41.54	164.77
Swin-B (cls)	91.47	17.56	41.18	162.02
SwinV2-B	92.14	19.60	30.91	117.69
SwinV2-S	54.08	12.19	31.32	118.77
SwinV2-T	32.70	7.42	54.58	198.20
ConvNext-B	92.80	17.90	73.09	185.69
ConvNext-S	54.57	11.17	74.75	246.71
ConvNext-T	32.93	6.94	105.02	336.47
ResNet101	48.23	10.54	66.84	238.02

**Table 7:** Parameter and FPS analysis with different backbones for *FaceXformer*.

formance, as shown in Table 7. Notably, for tasks such as regression (*reg*), classification (*cls*), and segmentation (*seg*), there is a minimal change in parameters and frames per second (FPS), which underscores the efficiency of the pipeline, as conventional face segmentation pipelines generally have more parameters and lower FPS than classification and regression pipelines. For example, Swin-B for segmentation, regression, and classification tasks demonstrates remarkable consistency in performance with FPS rates of 41.09, 41.54, and 41.18, respectively, while maintaining similar parameter counts around 91 million. In terms of overall FPS, ConvNext backbones outperform the others, with the ConvNext-T model achieving an 105.02 FPS, followed by ResNet101 and then Swin models.

## D In-the-wild Visualization

We randomly select images from the publicly available FFHQ [29] dataset and treat them as "in-the-wild" images, which were not used for training. We input the image along with multiple task tokens and present the qualitative results for all the tokens in Figure 5. We observe that *FaceXFormer* delivers competitive results across a variety of faces with variations in age, gender, race, head pose, background, lighting, etc.

## E Additional results

In this section, we expand upon the results presented in the main paper by providing class-wise F1 scores for face parsing on the LaPa [41] and CelebAMask-HQ [34] datasets. Additionally, we elaborate on the results of landmark detection across various subsets of these datasets, utilizing multiple metrics, as detailed in Table 10.

*FaceXFormer* achieves the highest F1-score for the "skin" class and the lowest for the "left-eyebrow" on the LaPa dataset. Similarly, on CelebAMask-HQ, it records the highest F1-score for "skin" and the lowest for the "right-eyebrow." From Tables 8 and 9, it is apparent that the class-wise segmentation performance

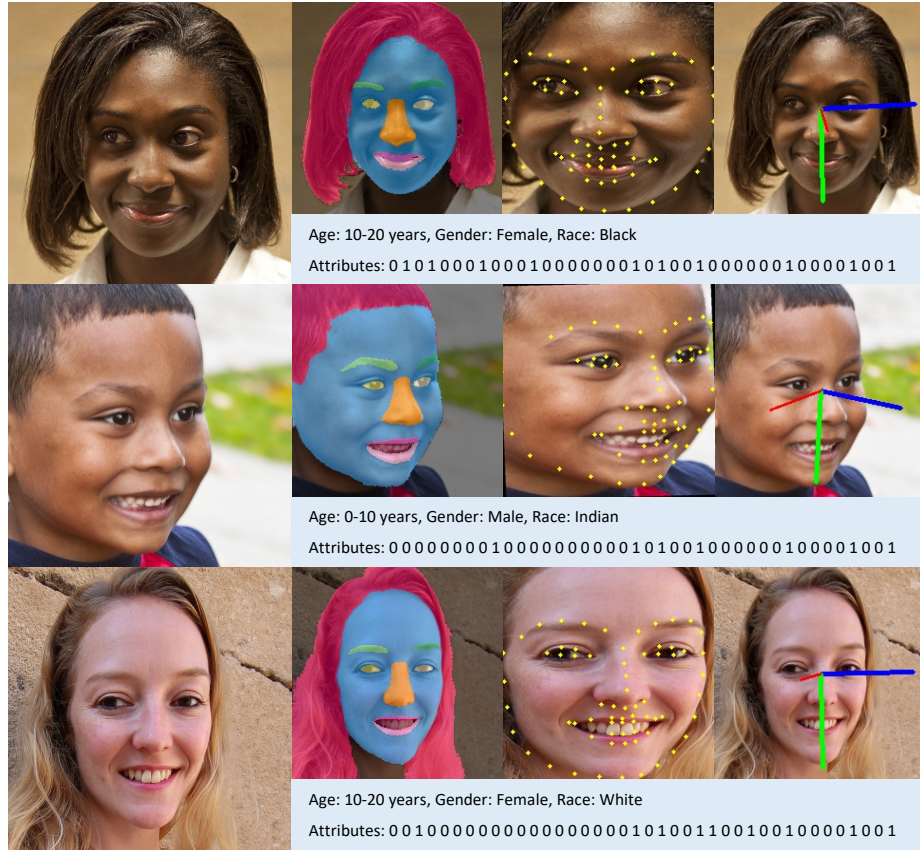


**Fig. 5:** Visualization of "in-the-wild" images queried for multiple task tokens. Attributes represent the 40 binary attributes defined in the CelebA [42] dataset, indicating the presence (1) or absence (0) of specific facial attributes.

ranking of *FaceXFormer* aligns with the pattern observed in other baseline models. Furthermore, *FaceXFormer* notably surpasses the recent state-of-the-art model, FP-LIIF [56], on the LaPa dataset, even with a lower input resolution.

From Table 10, we observe that *FaceXFormer* surpasses existing multi-task baseline models, particularly HyperFace and AllInOne, with a NME of 3.52 and 4.81 on the 300W [53] and WFLW [76] datasets, respectively. It also outperforms FaRL [88] on the 300W challenge set, achieving an NME of 5.13 compared to FaRL's 5.19. Additionally, *FaceXFormer* exceeds FaRL's performance on the WFLW dataset with a  $FR_{@10\%}$  of 4.56, compared to 5.72 for FaRL. Furthermore, its performance is on par with the current state-of-the-art model, demonstrating its capacity to generalize across various heterogeneous tasks without sacrificing performance in any specific task.



Method	Input Res.	Skin	Hair	Nose	LE	RE	LB	RB	LL	IM	UL	Mean
EAGR [65]	473	97.3	96.2	97.1	89.5	90.0	86.5	87.0	89.0	90.0	88.1	91.1
AGRNET [64]	473	97.7	96.5	97.3	91.6	91.1	89.9	90.0	90.1	90.7	88.5	92.3
DML-CSR [87]	473	97.6	96.4	97.3	91.8	91.5	90.4	90.4	89.9	90.5	88.0	92.4
FaRL [88]	512	97.1	93.0	97.2	91.6	91.5	90.1	89.6	89.1	89.4	87.2	91.6
FP-LIIF [56]	256	97.1	95.8	97.0	85.5	86.2	88.8	88.6	87.8	89.4	85.0	90.1
<b>FaceXFormer</b>	224	96.7	92.7	96.1	91.5	91.4	88.0	88.1	88.5	89.8	86.6	91.1

Table 8: Class-wise segmentation results on LaPa dataset

Method	Input Res.	Skin	Hair	Nose	LE	RE	LB	RB	LL	IM	UL	Mean
EAGR [65]	473	96.2	94.9	94.0	88.6	88.7	85.7	85.2	91.2	95.0	88.9	90.84
AGRNET [64]	473	96.5	95.2	93.9	88.7	89.1	85.5	85.6	91.1	92.0	89.1	90.67
DML-CSR [87]	473	95.7	94.5	93.9	89.4	89.6	85.5	85.7	91.0	91.8	87.4	90.45
FaRL [88]	512	96.1	94.9	93.8	89.0	89.0	85.3	85.4	90.0	91.7	88.1	90.34
FP-LIIF [56]	256	96.4	95.1	93.7	88.5	88.5	84.5	84.3	90.3	92.1	87.5	90.09
<b>FaceXFormer</b>	224	96.1	94.4	93.4	89.2	89.0	84.4	84.3	90.0	89.3	87.2	89.83

Table 9: Class-wise segmentation results on CelebAMask-HQ dataset

## F Datasets and Implementation Details

In this section, we detail the dataset characteristics and the augmentations applied to each dataset during training. *FaceXFormer* is trained using multiple datasets, which have varying sample sizes. Datasets with a larger number of images may dominate the training process and create bias. To mitigate this, we employ upsampling to ensure that each batch is represented by samples from every dataset. This is achieved by repeating the samples of smaller datasets through upsampling and then randomly sampling images from the upsampled set. The model is trained for 12 epochs with a total batch size of 384 and an initial learning rate of  $1e^{-4}$ , which decays by a factor of 10 at the 6<sup>th</sup> and 10<sup>th</sup> epochs. We use the AdamW optimizer with a weight decay of  $1e^{-5}$  for gradient updates.

Method	300W			WFLW								
	Full	Common	Challenge	Full			Pose	Exp	Ill	Makeup	Occl	Blur
	NME	NME	NME	NME	FR@10%	AUC@10%	NME	NME	NME	NME	NME	NME
Wing [17]	-	-	-	4.99	7.56	0.532	8.75	5.36	4.93	5.41	6.37	5.81
SBR [14]	4.10	3.28	7.58	-	-	-	-	-	-	-	-	-
DeCaFa [12]	3.39	2.93	5.26	4.62	4.84	0.563	8.11	4.65	4.41	4.63	5.74	5.38
HRNet [69]	3.32	2.87	5.15	4.60	4.64	-	7.94	4.85	4.55	4.29	5.44	5.42
STAR Loss [90]	2.87	2.52	4.32	4.02	2.32	0.605	6.76	4.27	3.97	3.84	4.80	4.58
FaRL [88]	3.35	2.90	5.19	4.80	5.72	0.545	8.78	5.09	4.74	4.99	6.01	5.35
HyperFace [51]	3.62	3.22	3.62	5.12	6.09	0.509	9.54	5.82	5.41	5.31	6.43	6.14
AllinOne [52]	4.52	3.98	6.67	6.90	15.4	0.391	13.4	7.91	7.05	7.42	8.53	7.95
<b>FaceXFormer</b>	3.52	3.13	5.13	4.81	4.56	0.530	8.80	5.67	5.12	5.07	6.00	5.86

Table 10: Landmarks detection results on various subsets of 300W and WFLW

### F.1 Face Parsing

We use LaPa [41] and CelebAMask-HQ [34] for training and evaluation of *FaceXFormer*. LaPa consists of around 22,000 facial images with 11-category pixel level map. CelebAMask-HQ contains 30,000 high-resolution face images annotated with 19 classes. To use both datasets for training, we take the intersection of class labels from both datasets. The classes used for training and evaluation include: skin, face, nose, left eye, right eye, left eyebrow, right eyebrow, upper lip, mouth, and lower lip. While training, we perform augmentations with random rotation ( $\pm 18^\circ$ ), random scaling ( $\pm 10\%$ ), random translation ( $1\% \times 224$ ), random horizontal flip (50%), random gray (10%), random Gaussian blur (10%) and random gamma adjustment(10%). We perform Tanh warping [40] on the LaPa dataset to ensure that the network can segment the whole face image while focusing on the face region. On CelebAMask-HQ, instead of Tanh-warping, we perform a resizing operation to  $224 \times 224$ , since all face images are already aligned.

### F.2 Landmarks Detection

We utilize the 300W [53] and WFLW [76] datasets for the training and evaluation of *FaceXFormer*. The 300W and WFLW datasets contain 3,148 and 7,500 images in their respective training sets. The 300W dataset includes 689 test images, categorized into three overlapping test sets: common (554 images), challenge (135 images), and full (689 images). It includes a large variety of identities, expression, illumination conditions, pose, occlusion, and face size. The images are annotated with 68 landmark points. The WFLW dataset includes 2,500 images for testing, each annotated with 98 landmark points. For the sake of unification, we convert the 98 landmarks to 68 landmarks using the standard landmark mapping. Additionally, it includes annotations for occlusion, head pose, makeup, illumination, blur, and expressions. We employ the 300VW [57] dataset for cross-dataset testing of multi-task methods. It offers three test sets: Category-A (well-lit conditions, comprising 31 videos with 62,135 frames), Category-B (mildly unconstrained conditions, with 19 videos containing 32,805 frames), and Category-C (challenging conditions, including 14 videos with 26,338 frames). We report the mean of these three categories. During training we apply augmentations such as random rotation ( $\pm 18^\circ$ ), random scaling ( $\pm 10\%$ ), random translation ( $5\% \times 224$ ), random horizontal flip (50%), random gray (20%), random Gaussian blur (30%), random occlusion (40%) and random gamma adjustment(20%). Additionally, we align the images using five landmarks points.

### F.3 Head Pose Estimation

We utilize the 300W-LP [93] and AFLW2000 [94] datasets, which contain approximately 122,000 samples and 2,000 images, respectively. We evaluate performance using the BIWI [16] dataset, comprising 15,678 images of 20 individuals (6 females and 14 males, with 4 individuals recorded twice). The head pose range covers about  $\pm 75^\circ$  yaw and  $\pm 60^\circ$  pitch. During training, we loosely crop the face

images based on the landmarks and apply augmentations, including random gray (10%), random Gaussian blur (10%), and random gamma adjustment(10%).

#### F.4 Attributes Recognition

We utilize the CelebA [42] dataset for training and the LFWA [74] dataset for cross-dataset evaluation of multi-task methods. CelebA comprises 202,599 facial images, each annotated with 40 binary labels that indicate various facial attributes such as hair color, attractive, bangs, big lips, and more. LFWA consists of 13,143 facial images, annotated with the same set of facial attributes. During training, we apply several augmentations, including random rotation ( $\pm 18^\circ$ ), random scaling ( $\pm 10\%$ ), random translation ( $1\% \times 224$ ), random horizontal flip (50%), random gray (10%), random Gaussian blur (10%), and random gamma adjustment(20%).

#### F.5 Age/Gender/Race Estimation

We employ the FairFace [28] and UTKFace [85] datasets for training, and the FFHQ [29] dataset for testing. FairFace comprises 108,501 images, balanced across seven racial groups: White, Black, Indian, East Asian, Southeast Asian, Middle Eastern, and Latino. The UTKFace dataset contains 20,000 facial images annotated with age, gender, and race. In our work, we follow the 'race-4' annotation scheme, categorizing individuals into five racial labels: White, Black, Indian, Asian, and Others. Age annotations are categorized into decade bins: 0-9, 10-19, 20-29, 30-39, 40-49, 50-59, 60-69, and over 70. Gender is annotated with two labels: male and female. During training, we apply augmentations, such as random rotation ( $\pm 18^\circ$ ), random scaling ( $\pm 10\%$ ), random translation ( $1\% \times 224$ ), random horizontal flip (50%), random gray (10%), random Gaussian blur (10%), and random gamma adjustment(20%).

#### F.6 Landmarks Visibility Prediction

We utilize the COFW [5] dataset, which is annotated with 29 landmarks for landmarks visibility prediction. Each landmark is associated with 29 binary labels that indicate its visibility. We loosely crop the faces and apply augmentations, including random horizontal flip (50%), random gray (10%), random Gaussian blur (10%), and random gamma adjustment(20%).